Published in final edited form as:
J Neurosci Res. 2008 February 1; 86(2): 448–456. doi:10.1002/jnr.21496.

Aquaporin-4 Water Channels in Enteric Neurons

Mia M. Thi[1], **David C. Spray**[1], and **Menachem Hanani**[2,*]

[1]Dominick P. Purpura Department of Neuroscience, Albert Einstein College of Medicine of Yeshiva University, Bronx, New York

[2]Laboratory of Experimental Surgery, Hebrew University—Hadassah Medical School and Hadassah University Hospital, Mount Scopus, Jerusalem, Israel

Abstract

Aquaporin-4 is a water channel predominantly found in astrocytes in the central nervous system and is believed to play a critical role in the formation and maintenance of the blood–brain barrier and in water secretion from the brain. As enteric glial cells were found to share several similarities with astrocytes, we hypothesized that enteric glia might also contain aquaporin-4. We used immunohistochemistry to identify aquaporin-4 in the myenteric and submucosal plexuses of the mouse and the rat colon. We found that sub-populations of neurons in both enteric plexuses were positively labeled for human aquaporin-4. Double staining of the enteric ganglia with antibodies to the neuronal marker neurofilament–heavy chain 100 and to aquaporin-4 showed that a minority of myenteric neurons were aquaporin-4 positive (about 12% in the mouse and 13% in the rat). In contrast, in the submucosal plexus significant numbers of neurons were positive for aquaporin-4 (about 79% in both the mouse and the rat). Double labeling for aquaporin-4 and for the glial marker glial fibrillary acidic protein verified that glial cells were not immunoreactive to aquaporin-4. We further confirmed our findings with additional aquaporin-4 antibodies and Western blot analysis. We found that, in addition to expressing aquaporin-4, the myenteric plexus and, to a greater extent, the submucosal plexus both expressed aquaporin-1. We conclude that neurons rather than glial cells contain aquaporin-4 in the colonic enteric plexuses. It is known that submucosal neurons control transport processes in the intestinal mucosa, and the high percentage of aquaporin-4-postive sub-mucosal neurons suggests that aquaporin-4 contributes to this function.

Keywords

AQP4; AQP1; myenteric plexus; submucosal plexus; mouse; rat

The discovery of water channels, or aquaporins (AQPs), has had important implications for understanding both the normal function and pathological conditions of many organ systems (Agre et al., 2002). The identification of AQPs in the gastrointestinal (GI) tract is of particular interest, as this system handles the transport of large amounts of water. Several studies have shown that the intestinal mucosa has most types of AQPs (Ma and Verkman, 1999; Mobasheri et al., 2004). For example, the rat colonic mucosa contains AQP4 (Ma and Verkman, 1999), and the human small intestinal mucosa contains AQP3 and AQP10 (Mobasheri et al., 2004).

Aquaporins have also been detected in the nervous system, and are particularly abundant in astrocytes (Nielsen et al., 1997; Amiry-Moghaddam and Ottersen, 2003). AQP4 is located in

*Correspondence to: Menachem Hanani, Laboratory of Experimental Surgery, Hadassah University Hospital, Mount Scopus, Jerusalem 91240, Israel. E-mail: E-mail: hananim@cc.huji.ac.il.

astrocytic end-feet in membranes that contact capillaries and pia, that is, in regions where the exchange of water between the brain and extracerebral liquids takes place. It was therefore suggested that AQP4 may play a role in the regulation of water homeostasis in the central nervous system (Amiry-Moghaddam and Ottersen, 2003; Nicchia et al., 2004). In addition, Abbott et al. (2006) suggested that AQP4 may have a role in the functions of the blood–brain barrier under both normal and pathological conditions. Numerous reports have explored the roles of aquaporins in the CNS (Venero et al., 2001; Lehmann et al., 2004; Manley et al., 2004), yet their roles in the GI nervous system have not been fully investigated. The GI tract contains a highly developed intrinsic nerve network—the enteric nervous system (ENS; Kunze and Furness, 1999; Grundy and Schemann, 2005). In addition to neurons, enteric ganglia contain many specialized glial cells termed enteric glia. These cells have some resemblance to astrocytes, both biochemically (Jessen and Mirsky, 1983; Ruhl, 2005) and morphologically (Hanani and Reichenbach, 1994). Despite these similarities, there is no information on the presence of AQP4 in enteric glia. As enteric glia also form part of the external surface of the enteric ganglia and make contact with blood vessels (Gabella, 1994; Hanani and Reichenbach, 1994), we hypothesized that these cells might contain AQP4. Using immunofluorescence labeling, we found that enteric glia in mouse and rat colon are actually devoid of this protein and instead that a significant proportion of the neurons were AQP4- and AQP1-positive. It was recently demonstrated that there is a similar neuronal distribution of AQP1 in the rat small intestine (Nagahama et al., 2006).

MATERIALS AND METHODS

Tissues Preparation

Twenty adult male C57BL/6J mice (Charles River Laboratories, Wilmington, MA) and three adult female Sprague Dawley rats (Taconic, NY) were sacrificed by overdose with isoflurane (Abbott Laboratories, Abbott Park, IL). All procedures were performed according to a protocol approved by the Institute for Animal Studies of the Albert Einstein College of Medicine, Bronx, New York, in accordance with NIH Guidelines. The abdominal wall was opened, and the distal colon was removed and placed in phosphate-buffered saline (PBS; pH 7.4) at 4°C. The colon was opened along the mesenteric border, and the mucosa and submucosa were removed under a dissecting microscope and placed in PBS. We used two types of preparation: the external muscle layers with the myenteric plexus and the submucosa with the submucosal plexus. Tissues were fixed for 2 hr in 4% paraformaldehyde in PBS and then washed four times in PBS.

Immunofluorescence and Confocal Microscopy

Whole-mount tissue preparations were permeabilized with 0.25% Triton X-100 in PBS for 10 min and blocked with 1% bovine serum albumin (Sigma-Aldrich, St. Louis, MO) in PBS for 1 hr at room temperature. They were then incubated with primary antibodies for 72 hr at 4°C followed by a 2-hr incubation with secondary antibody at room temperature with intervening washes. The antibodies used were goat polyclonal antibody against human AQP4 (AQP4-C19; Santa Cruz Biotechnology, Santa Cruz, CA), 1:50; rabbit polyclonal antibody against rat AQP4 (A5971; Sigma-Aldrich), 1:50; rabbit polyclonal antibody against rat AQP4 (AQP41A; Alpha Diagnostic International, San Antonio, TX), 1:50; rabbit polyclonal antibody against rat AQP1 (AQP11-A; Alpha Diagnostic International), 1:100; rabbit polyclonal antibody against human neurofilament–heavy chain 100 [NF-H (H100); Santa Cruz Biotechnology], 1:100; and monoclonal antibody against glial fibrillary acidic protein (G3893; Sigma-Aldrich), 1:400. Secondary antibodies (Invitrogen, Carlsbad, CA) conjugated to Alexa 488 and 594 were used at ratios between 1:400 and 1:600. For AQP4 competition studies, blocking peptide corresponding to the carboxy terminus of human AQP4 (Santa Cruz Biotechnology) was incubated with AQP4 antibody (5:1 ratio) for 2 hr prior to a 72-hr incubation with tissue

samples. Tissues were mounted on slides with mounting medium containing glycerol, poly (vinyl alcohol), *n*-propyl gallate, and the nucleophilic dye DAPI. They were examined and photographed on a Nikon Eclipse TE300 microscope using a Spot-RT digital camera (Diagnostic Instruments, Sterling Heights, MI).

The tissues were also examined with an Olympus Fluo-View FV500 Laser Scanning Confocal Microscope (Olympus, Center Valley, PA) using a ×40 water-immersion objective. Images were taken serially from top to bottom of each image field using a *z*-plane motorized substage. The upper and lower *z*-axis positions were selected so that the entire thickness of either the submucosal plexus or the myenteric plexus was imaged in each series. Image stacks (13–37 optical sections per stack) of tissue samples were collected at 0.62-μm *z*-axis steps. AQP4 distributions in confocal images were analyzed using Imaris software (Bitplane AG, MN).

Western Blot Analysis

Tissues of adult C57BL/6J brain, colon external muscle (containing myenteric plexus), and submucosa (containing submucosal plexus) were collected from the same mice. The astrocytes were dissociated from neonatal C57BL/6J mice. Samples were lysed and sonicated in buffer containing 1 mM sodium bicarbonate, 1 mM sodium orthovanadate, 5 mM EDTA, and 2 mM PMSF as described in Thi et al. (2003). Samples were prepared at room temperature with loading buffer containing 4% SDS, 10% glycerol, 125 mM Tri-HCL, and 100 mM dithiothreitol and were loaded onto 12% SDS-PAGE gels for separation and electrophoretically transferred to nitrocellulose membranes (Whatman, Dassel, Germany). The membranes were probed with primary polyclonal antibodies to goat antihuman AQP4 (AQP4-C19; Santa Cruz Biotechnology), 1:1,000; rabbit antirat AQP4 (A5971; Sigma-Aldrich), 1:1000; and rabbit antirat AQP4 (AQP41A; Alpha Diagnostic International), 1:250; followed by secondary antibody incubation with horseradish peroxidase (HP)–conjugated antigoat IgG and antirabbit IgG (Santa Cruz Biotechnology, Santa Cruz, CA). The protein bands were detected using an Amersham ECL detection kit (Amersham Biosciences, Piscat-away, NJ) and exposed on Fuji X-ray film.

Statistical Analysis

Immunolabeled cells were counted in randomly selected fields using an Nikon Eclipse microscope. Means were compared using two-tailed *t* tests and nonparametric tests (Wilcoxon matched-pairs test); differences with a P value < 0.05 were considered statistically significant.

RESULTS

Mouse Colon

Low-magnification (×10 objective) micrographs of the myenteric plexus colabeled with antibodies to AQP4 and the neuronal marker NF-H (H100) revealed that the myenteric plexus in the mouse colon contained a large number of AQP4-positive nerve fibers and a fair number of labeled neuronal somata (arrows and arrowheads, Fig. 1). As shown in Figure 2A,D, confocal image analysis of the myenteric and submucosal plexuses confirmed that neurons (arrowheads) as well as nerve fibers (arrows) were distinctly stained for AQP4. AQP4-positive neurons were more abundant in the submucosal plexus than in the myenteric plexus. In a small percentage of myenteric ganglia (14 ± 4%), none of the neuronal somata were AQP4-positive, but AQP4-positive nerve fibers were still very conspicuous, as illustrated in Figure 2B. In the submucosal plexus, AQP4-positive nerve fibers were seen close to submucosal blood vessels (Fig. 2E), consistent with this protein being in submucosal neurons. Preincubating the tissues with the peptide to which AQP4 antibody was generated completely eliminated both somata and fiber staining in both plexuses, validating AQP4 expression (Fig. 2C,F).

To analyze the proportion of AQP4-positive neurons in the ganglia, we carried out a double-labeling study using AQP4, and NF-H (H100) antibodies to label the neurons. As shown in Table I, analysis of 137 ganglia from five mice showed that AQP4-positive neurons made up 12 ± 1% of the NF-H-positive neurons in the myenteric plexus. The AQP4-positive nerve fibers were very brightly stained in most cases (Fig. 3A, arrows). As clearly shown in Figure 3A, the AQP4-positive neurons were monopolar, and many had short, broad processes, typical for enteric Dogiel type I neurons, indicated by an asterisk (Gabella, 1994). Dogiel II neurons (smooth somata with more than one long process) were not stained for AQP4. Analysis of cross-sectional views of confocal images revealed a diffuse distribution of AQP4 in the cell bodies of neurons, as shown in Figure 3D. Occasional colocalization of AQP4 and NF-H in some neurons was also detected (Fig. 3C,D, *XZ* and *YZ* views). Moreover, we observed that in most cases AQP4 was uniformly distributed along nerve fibers (Fig. 3E, *XZ* and *YZ* views), and in a few cases we detected colocalization with NF-H (Fig. 3F, *XZ* and *YZ* views).

Ganglia in the submucosal plexus are smaller than those in the myenteric plexus; indeed, there were fewer NF-positive neurons in the submucosal plexus than in the myenteric plexus. However, in contrast with that in the myenteric plexus, the proportion of AQP4-positive neurons was very high (79 ± 5% of the total number of neurons), as determined by counting the NF-positive cells from 148 ganglia (Table I). As shown in Figure 3G–I, the submucosal plexus consists of two distinct layers (indicated by arrowheads and arrows), with the pattern of AQP staining similar in both layers. Cross-sectional analyses of confocal images showed abundant colocalization of AQP4 and NF-H in neurons of the submucosal plexus (Fig. 3J). The nerve fiber strands in the submucosal plexus also showed uniform distribution of AQP4 and occasional colocalization of AQP4 with NF-H (Fig. 3K,L).

It is well established that enteric glia can be identified using staining for the glial marker glial fibrillary acidic protein (GFAP; Jessen and Mirsky, 1983; Ruhl, 2005). To test whether glial cells in the mouse colon were also labeled for AQP4, we carried out a double-labeling study for AQP4 and GFAP. As can be seen in Figure 4A–C, the pattern of staining for GFAP conformed to that of previous reports on glial cells (Jessen and Mirsky, 1983), and the only cells that were AQP4 positive in the myenteric plexus were the neurons. Further cross-sectional analysis showed that AQP4-positive neurons were surrounded by a dense network of glial cell bodies and their processes (Fig. 4D, *XZ* and *YZ* views). In addition, we observed some apparent colocalization of AQP4 and GFAP where the nerve fibers came into close contact with glia cell processes (Fig. 4F, *XZ* view). However, in these rare cases it was not possible to resolve unambiguously whether the processes containing AQP4 were GFAP-positive.

Double labeling for GFAP and AQP4 in the submucosal plexus clearly showed that enteric glia were not AQP4 positive (Fig. 4G–K). However, as was the case with nerve fibers in the myenteric plexus, nerve fibers in the submucosal plexus exhibited colocalization of AQP4 and GFAP in the regions where they were in close contact with fine processes of glial cells, as shown in Figure 4L. This colocalization of AQP4 and GFAP in regions of contact with neurons could be a result of either induced low-level expression in glia in contact with nerve processes or intermingling thin processes of neurons and glia, rendering cellular localization ambiguous.

In some instances, AQP4-positive nerve fibers were observed in both the longitudinal and circular muscle layers, as shown in serial confocal images of Figure 5. We found AQP4-positive varicose nerve fibers in the longitudinal muscle layer, as shown in Figure 5A (arrowheads). Furthermore, we observed some AQP4- and NF-H-positive nerve bundles between two ganglia and other varicose nerve fibers (Fig. 5B, arrowheads) that were situated 2.74 μm within the layer (Fig. 5A). We also noted that AQP4-positive nerve fibers were present in the circular muscle layer (Fig. 5B).

To substantiate our findings, we performed additional staining using AQP4 antibodies raised in rabbit against rat AQP4 (from Sigma-Aldrich and Alpha Diagnostic International). In the myenteric plexus we observed diffuse AQP4 puncta in the neurons (arrowheads) and alongside some nerve fibers (arrows), as shown in Figure 6A,D. Both AQP4 antibodies exhibited similar distributions of AQP4 in neurons as well as in nerve fibers. In addition, we used GFAP immunolabeling to identify the glial cell network (Fig. 6B–E) and to confirm that AQP4-labeled cells were neurons. Our results clearly indicated that some neurons and nerve fibers in the myenteric plexus indeed expressed AQP4. Moreover, in the submucosal plexus we detected abundant expression of AQP4 in numerous neurons (arrowheads) and in some nerve fibers (arrows), as shown in Figure 6G,J. Similar to the staining with human AQP4 antibody, illustrated in Figure 3G and Figure 4G, most neurons in the submucosal plexus were positively labeled for rat AQP4. GFAP expression in the same fields (Fig. 6G,J) demonstrated that only neurons were labeled for AQP4; there was some colocalization of AQP4 and GFAP in the regions where AQP4-positive nerve fibers and fine processes of glial cells were in very close contact, as shown in Figure 6H–K. To validate recognition of similar structures by different AQP4 antibodies, we carried out double labeling for AQP4 using antibodies from Santa Cruz Biotechnology and Sigma-Aldrich. In the myenteric plexus, there was some degree of colocalization in the neurons and much higher colocalization in the nerve fibers. In the submucosal plexus, we found a very high degree of colocalization of structures stained by the antibodies in both neurons and nerve fibers (data not shown).

To assess whether colonic plexuses express AQP1, as reported for the small intestine, we performed double labeling of AQP1/AQP4 and AQP1/GFAP. As shown in Figure 7A,B,D, some colonic myenteric neurons (asterisks) and nerve fibers (group of arrows) were more faintly positive for AQP1 compared to AQP4-positive neurons (arrowheads) and nerve fibers. Blood vessels (x) were vividly positive for AQP1. There was very little or no colocalization of AQP1 and AQP4 in the myenteric plexus (Fig. 7C). Double labeling with AQP1 and GFAP showed that myenteric glia did not express AQP1; there was some colocalization in the region where glia cell processes and AQP1-positive nerve fibers intertwine with each other, indicated by an arrow (Fig. 7F). In contrast, submucosal neurons (arrowheads) and nerve fibers (arrows) not only coexpressed AQP1 and AQP4 but also colocalized (single arrows) to some degree, as shown in Figure 7G–I. Often we observed that nerve fibers were positive for AQP4 (single arrows) and AQP1 (group of arrows). Double labeling with AQP1 and GFAP in the submucosal plexus demonstrated that only neurons (arrowheads) were AQP1 positive (Fig. 7J–L). There were quite a few cases of colocalization of AQP1 and GFAP at locations where nerve fibers and glial cell processes were in close vicinity to each other, as shown in Figure 7L (single arrows).

Rat Colon

As a further test of the generality of our findings, we carried out AQP4 immunofluorescence studies in the rat colon, which showed patterns of AQP4 distribution very similar to those obtained in the mouse colon. Similar to the mouse myenteric plexus, about 13 ± 4% of myenteric ganglia in rats were devoid of AQP4-positive neurons; only AQP4-positive nerve fibers were present in those ganglia. As shown in Figure 8A,D, many neurons (arrowheads) and nerve fibers (arrows) in both myenteric and submucosal plexuses were positively labeled for AQP4. Colabeling of the same cell fields with NF-H, as shown in Figure 8A,D, further confirmed that AQP4 was indeed present in neurons and nerve fibers (Fig. 8B,C,E,F). Analysis of 99 myenteric ganglia from three rats indicated that 13 ± 2% of NF-H-labeled neurons were positively labeled for AQP4, as listed in Table I. On the other hand, in the submucosal plexus, the percentage of AQP4-positive neurons relative to the percentage of NF-H-labeled neurons was very high, 79 ± 2%.

AQP4 Expression in the Colon

We also performed Western blots to analyze whether AQP4 was present in ganglia and nerve fibers of the mouse colon. We used tissue samples of brain, myenteric, and submucosal plexuses from the same animals. As demonstrated in Figure 9, we performed parallel Western blot analyses using brain and astrocytes as positive controls with (A) goat polyclonal antibody against human AQP4 (Santa Cruz Biotechnology), (B) rabbit polyclonal antibody against rat AQP4 (Sigma-Aldrich), and (C) rabbit polyclonal antibody against rat AQP4 (Alpha Diagnostic International) to determine whether AQP4 was present in the myenteric and submucosal plexuses. Previous studies have shown that AQP4 displays multiple bands (either 30 and 32 kDa or 32 and 34 kDa) in Western blot analysis (Frigeri et al., 1998;Neely et al., 1999). Those doublets are the most abundant forms of AQP4. There are two additional bands (around 36 and 38 kDa) that were scarcely expressed, mainly in the cerebellum, spinal cord, and renal inner medulla (Neely et al., 1999). In addition, Neely et al. (1999) showed that when AQP4 is run on gels, it displays monomers around 30 kDa, dimers around 60 kDa, and trimers around 100 kDa. Our results confirmed that each of these antibodies recognized doublets (~31 kDa) in brain, astrocytes, and ganglia and nerve fibers of the myenteric and submucosal plexuses. We consider the band at about 75 kDa to be a nonspecific band and to be unrelated to AQP4. As expected, levels of AQP4 in the myenteric and submucosal plexuses were low compared to the amounts expressed in brain and astrocytes. Stronger bands were obtained for myenteric tissue because the submucosal plexus is much sparser than the myenteric plexus. Although there were notably fewer AQP4-positive neurons in the myenteric plexus than in the submucosal plexus, abundant AQP4 expression in the nerve fibers most likely contributed to the higher expression of this protein in the myenteric plexus. This difference most likely offset the higher percentage of AQP4 content in the submucosal plexus.

DISCUSSION

Enteric glia and astrocytes share several similarities, and the hypothesis investigated in the present work was that, like astrocytes, enteric glia would express AQP4. The results described above clearly refuted this hypothesis. This outcome was somewhat unexpected but not altogether surprising because these two cell types differ in a number of details. For example, enteric glia differ from astrocytes in their responses to certain cytokines (Ruhl et al., 2001), and unlike astrocytes, their development requires the presence of neuregulins (Ruhl, 2005). Our findings suggest that at least some of the functions of enteric glia may be different than those of astrocytes. The presence of AQP4 and AQP1 in a substantial population of enteric neurons indicates that these cells have water transport–related functions, which need to be explored.

It has been suggested that AQP4 in astrocytes contributes to the exchange of water between the brain and blood vessels and plays a role in astrocyte migration during glial scar formation (Amiry-Moghaddam and Ottersen, 2003; Saadoun et al., 2005). Unlike most CNS regions, the ENS is not protected by a blood–brain barrier (Jacobs, 1977; Allen and Kiernan, 1994). Therefore, it might be suggested that AQP4 is absent in enteric glia because enteric ganglia do not have barrier functions.

Recently, AQP1 was identified in enteric neurons of the rat small intestine (Nagahama et al., 2006). The neurons appeared to have Dogiel I morphology, as we found for the AQP4-containing neurons in the mouse colon. In contrast, in the human esophagus, enteric neurons were found to be AQP4- and AQP1-negative, whereas enteric glia were AQP1 positive but AQP4 negative (Gao et al., 2006). Whether this is a peculiarity of the esophagus or of the human ENS remains to be investigated. The AQP1 results obtained for the rat myenteric plexus in a previous study (Nagahama et al., 2006) are very similar to ours for AQP4, with approximately 12% of mouse myenteric neurons and 13% of rat myenteric neurons being

AQP4 positive. However, the proportion of AQP4-positive submucosal neurons found in the mouse and rat colon was very large, nearly 80% of the neurons in both mice and rats, whereas only “a few” AQP1-labeled neurons were observed in the rat small intestine (Nagahama et al., 2006). Our partial assessment of AQP1 expression in the colonic plexuses suggests that AQP1 is more abundantly expressed in the submucosal plexus than in the myenteric plexus. This further indicates the difference in the distributions of AQP1 and AQP4 in the rat small intestine and mouse colon. Previous studies of the colon have identified AQP4 expression only in epithelial cells; additional studies with AQP4-knockout mice found that AQP4 seems to play a role in colonic fluid absorption through proximal colonic surface epithelium (Wang et al., 2000).

It is likely that the enteric nervous system plays a key role in body fluid homeostasis by regulating the transport of ions across intestinal epithelium (Cooke, 1989). There is strong evidence that submucosal neurons innervate the intestinal mucosa and participate in the control of transport processes in the GI tract (Xue et al., 2007). As aquaporins clearly contribute to transport processes in various tissues (Agre et al., 2002), AQP4 and AQP1 in submucosal neurons may contribute to this function. One key reason for enteric neurons to express AQP4 and AQP1 may be to enable them to monitor changes in osmotic pressure in the colon. Thus it is possible that AQP4- and AQP1-positive neurons in the myenteric and submucosal plexuses participate in reflexes that control water movement across the mucosa. Our observation of AQP4-labeled nerve fibers in both longitudinal and circular muscle implies that neurons sensitive to osmolarity changes can directly influence muscle activity.

One clear distinction between AQP4 and AQP1 staining was the presence of AQP1, but not AQP4, in intestinal blood vessels. This was noted previously for the rat small intestine (Nagahama et al., 2006) and was shown in the present study for the rat and mouse large intestine (Fig. 7). AQP1 is known to be present in endothelial cells in intestinal blood vessels (Ma and Verkman, 1999), which is consistent with these observations. These results show that there is a clear differential distribution of different aquaporins.

To our knowledge this is the first report of the presence of AQP4 in neurons of the adult enteric nervous system. AQP4 was detected in horizontal cells in the newborn mouse retina, but on postnatal day 15 the AQP4 immunoreactivity in these cells disappeared and was displayed in Müller cells (Bosco et al., 2005). It will be worthwhile finding out whether the expression of AQP4 in the enteric nervous system undergoes similar postnatal changes. In addition, as little attention has been paid to the contribution of aquaporins to water transport mechanisms in the GI tract, it will also be valuable to carry out a comprehensive study of the distribution of various aquaporins in all regions of the GI tract in rodents and other species.

ACKNOWLEDGMENTS

We thank Drs. Antonio Frigeri and Grazia Paola Nicchia [Department of General and Environmental Physiology and Centre of Excellence in Comparative Genomics (CEGBA), University of Bari, Italy] and Dr. Sylvia O. Suadicani (Dominick P. Purpura Department of Neuroscience, AECOM) for helpful discussions.

Contract grant sponsor: U.S.–Israel Binational Science Foundation (BSF); Contract grant number: 2003262; Contract grant sponsor: NIH; Contract grant numbers: MH65495, NS041282 and HL082130.

REFERENCES

Abbott NJ, Ronnback L, Hansson E. Astrocyte-endothelial interactions at the blood–brain barrier. Nat Rev Neurosci 2006;7:41–53. [PubMed: 16371949]

Agre P, King LS, Yasui M, Guggino WB, Ottersen OP, Fujiyoshi Y, Engel A, Nielsen S. Aquaporin water channels—from atomic structure to clinical medicine. J Physiol 2002;542:3–16. [PubMed: 12096044]

Allen DT, Kiernan JA. Permeation of proteins from the blood into peripheral nerves and ganglia. Neuroscience 1994;59:755–764. [PubMed: 8008217]

Amiry-Moghaddam M, Ottersen OP. The molecular basis of water transport in the brain. Nat Rev Neurosci 2003;4:991–1001. [PubMed: 14682361]

Bosco A, Cusato K, Nicchia GP, Frigeri A, Spray DC. A developmental switch in the expression of aquaporin-4 and Kir4.1 from horizontal to Muller cells in mouse retina. Invest Ophthalmol Vis Sci 2005;46:3869–3875. [PubMed: 16186376]

Cooke HJ. Role of the "little brain" in the gut in water and electrolyte homeostasis. FASEB J 1989;3:127–138. [PubMed: 2464517]

Frigeri A, Nicchia GP, Verbavatz JM, Valenti G, Svelto M. Expression of aquaporin-4 in fast-twitch fibers of mammalian skeletal muscle. J Clin Invest 1998;102:695–703. [PubMed: 9710437]

Gabella, G. Structure of muscles and nerves of the gastrointestinal tract. In: Johnson, LR., editor. Physiology of the gastrointestinal tract. New York: Raven; 1994. p. 751-793.

Gao H, He C, Fang X, Hou X, Feng X, Yang H, Zhao X, Ma T. Localization of aquaporin-1 water channel in glial cells of the human peripheral nervous system. Glia 2006;53:783–787. [PubMed: 16534779]

Grundy D, Schemann M. Enteric nervous system. Curr Opin Gastroenterol 2005;21:176–182. [PubMed: 15711209]

Hanani M, Reichenbach A. Morphology of horseradish peroxidase (HRP) –injected glial cells in the myenteric plexus of the guinea-pig. Cell Tissue Res 1994;278:153–160. [PubMed: 7954696]

Jacobs JM. Penetration of systemically injected horseradish peroxidase into ganglia and nerves of the autonomic nervous system. J Neuro-cytol 1977;6:607–618.

Jessen KR, Mirsky R. Astrocyte-like glia in the peripheral nervous system: an immunohistochemical study of enteric glia. J Neurosci 1983;3:2206–2218. [PubMed: 6138397]

Kunze WA, Furness JB. The enteric nervous system and regulation of intestinal motility. Annu Rev Physiol 1999;61:117–142. [PubMed: 10099684]

Lehmann GL, Gradilone SA, Marinelli RA. Aquaporin water channels in central nervous system. Curr Neurovasc Res 2004;1:293–303. [PubMed: 16181079]

Ma T, Verkman AS. Aquaporin water channels in gastrointestinal physiology. J Physiol 1999;517:317–326. [PubMed: 10332084]

Manley GT, Binder DK, Papadopoulos MC, Verkman AS. New insights into water transport and edema in the central nervous system from phenotype analysis of aquaporin-4 null mice. Neuroscience 2004;129:983–991. [PubMed: 15561413]

Mobasheri A, Shakibaei M, Marples D. Immunohistochemical localization of aquaporin 10 in the apical membranes of the human ileum: a potential pathway for luminal water and small solute absorption. Histochem Cell Biol 2004;121:463–471. [PubMed: 15221416]

Nagahama M, Ma N, Semba R, Naruse S. Aquaporin 1 immunoreactive enteric neurons in the rat ileum. Neurosci Lett 2006;395:206–210. [PubMed: 16309835]

Neely JD, Christensen BM, Nielsen S, Agre P. Heterotetrameric composition of aquaporin-4 water channels. Biochemistry 1999;38:11156–11163. [PubMed: 10460172]

Nicchia GP, Nico B, Camassa LM, Mola MG, Loh N, Dermietzel R, Spray DC, Svelto M, Frigeri A. The role of aquaporin-4 in the blood-brain barrier development and integrity: studies in animal and cell culture models. Neuroscience 2004;129:935–945. [PubMed: 15561409]

Nielsen S, Nagelhus EA, Amiry-Moghaddam M, Bourque C, Agre P, Ottersen OP. Specialized membrane domains for water transport in glial cells: high-resolution immunogold cytochemistry of aquaporin-4 in rat brain. J Neurosci 1997;17:171–180. [PubMed: 8987746]

Ruhl A. Glial cells in the gut. Neurogastroenterol Motil 2005;17:777–790. [PubMed: 16336493]

Ruhl A, Franzke S, Collins SM, Stremmel W. Interleukin-6 expression and regulation in rat enteric glial cells. Am J Physiol Gastrointest Liver Physiol 2001;280:G1163–G1171. [PubMed: 11352809]

Saadoun S, Papadopoulos MC, Watanabe H, Yan D, Manley GT, Verkman AS. Involvement of aquaporin-4 in astroglial cell migration and glial scar formation. J Cell Sci 2005;118:5691–5698. [PubMed: 16303850]

Thi MM, Kojima T, Cowin SC, Weinbaum S, Spray DC. Fluid shear stress remodels expression and function of junctional proteins in cultured bone cells. Am J Physiol Cell Physiol 2003;284:C389–C403. [PubMed: 12388096]

Venero JL, Vizuete ML, Machado A, Cano J. Aquaporins in the central nervous system. Prog Neurobiol 2001;63:321–336. [PubMed: 11115728]

Wang KS, Ma T, Filiz F, Verkman AS, Bastidas JA. Colon water transport in transgenic mice lacking aquaporin-4 water channels. Am J Physiol Gastrointest Liver Physiol 2000;279:G463–G470. [PubMed: 10915657]

Xue J, Askwith C, Javed NH, Cooke HJ. Autonomic nervous system and secretion across the intestinal mucosal surface. Auton Neurosci 2007;133:55–63. [PubMed: 17336595]

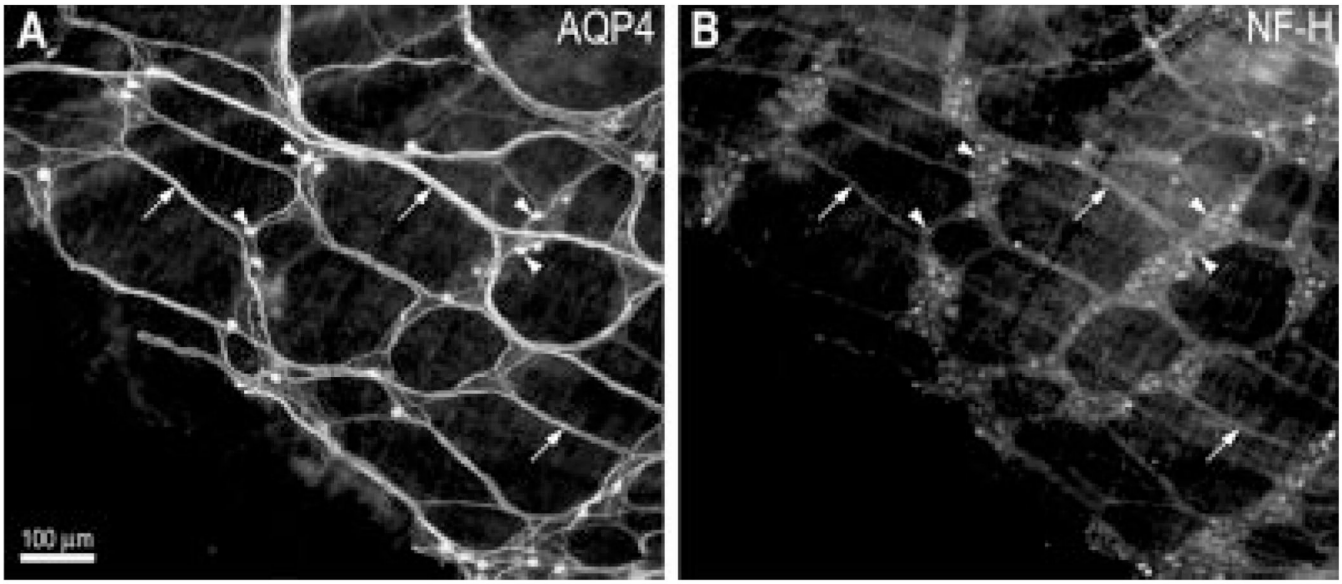

Fig. 1.

General pattern of AQP4 distribution in the myenteric plexus of the mouse colon obtained using goat polyclonal antibody against human AQP4 (Santa Cruz Biotechnology). **A**: Low-magnification micrograph showing AQP4-positive neurons (arrowheads) and nerve fibers (arrows). **B**: The same field as in A showing staining for the neuronal marker NP-H. Note the similar pattern obtained for both labels. Scale bar = 100 µm.

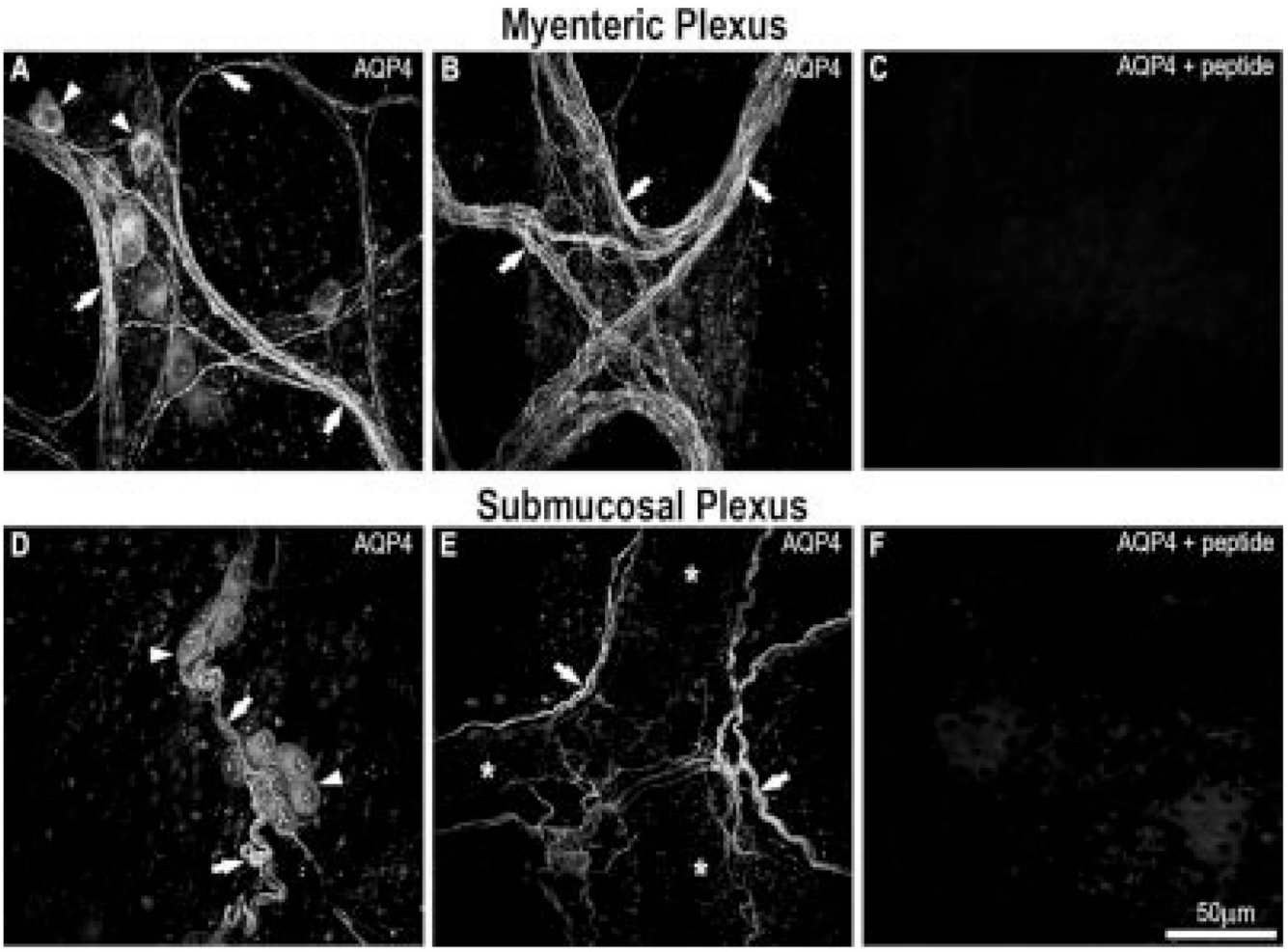

Fig. 2.

Confocal microscopy analysis of the myenteric plexus (A–C) and the submucosal plexus (D–F) in the mouse colon using goat polyclonal antibody against human AQP4 (Santa Cruz Biotechnology). **A**: Typical stacked image of ganglia in the myenteric plexus showing AQP4-containing neurons (arrowheads) and internodal nerve fiber strands (arrows). **B**: Ganglion in the myenteric plexus where only nerve fibers (arrows) were labeled for AQP4. **C**: Competition study in myenteric plexus, using blocking peptide corresponding to the carboxy terminus of AQP4, completely blocked AQP4 labeling of both neurons and nerve fibers. **D**: Typical stacked image of ganglia in the submucosal plexus showing AQP4-containing neurons (arrowheads) and internodal nerve fiber strands (arrows). **E**: AQP4-positive nerve fibers (arrows) were commonly seen around blood vessels in the submucosal plexus (asterisks). **F**: Competition study in submucosal plexus, using blocking peptide corresponding to the carboxy terminus of AQP4, completely blocked AQP4 labeling of both neurons and nerve fibers. Scale bar = 50 μm.

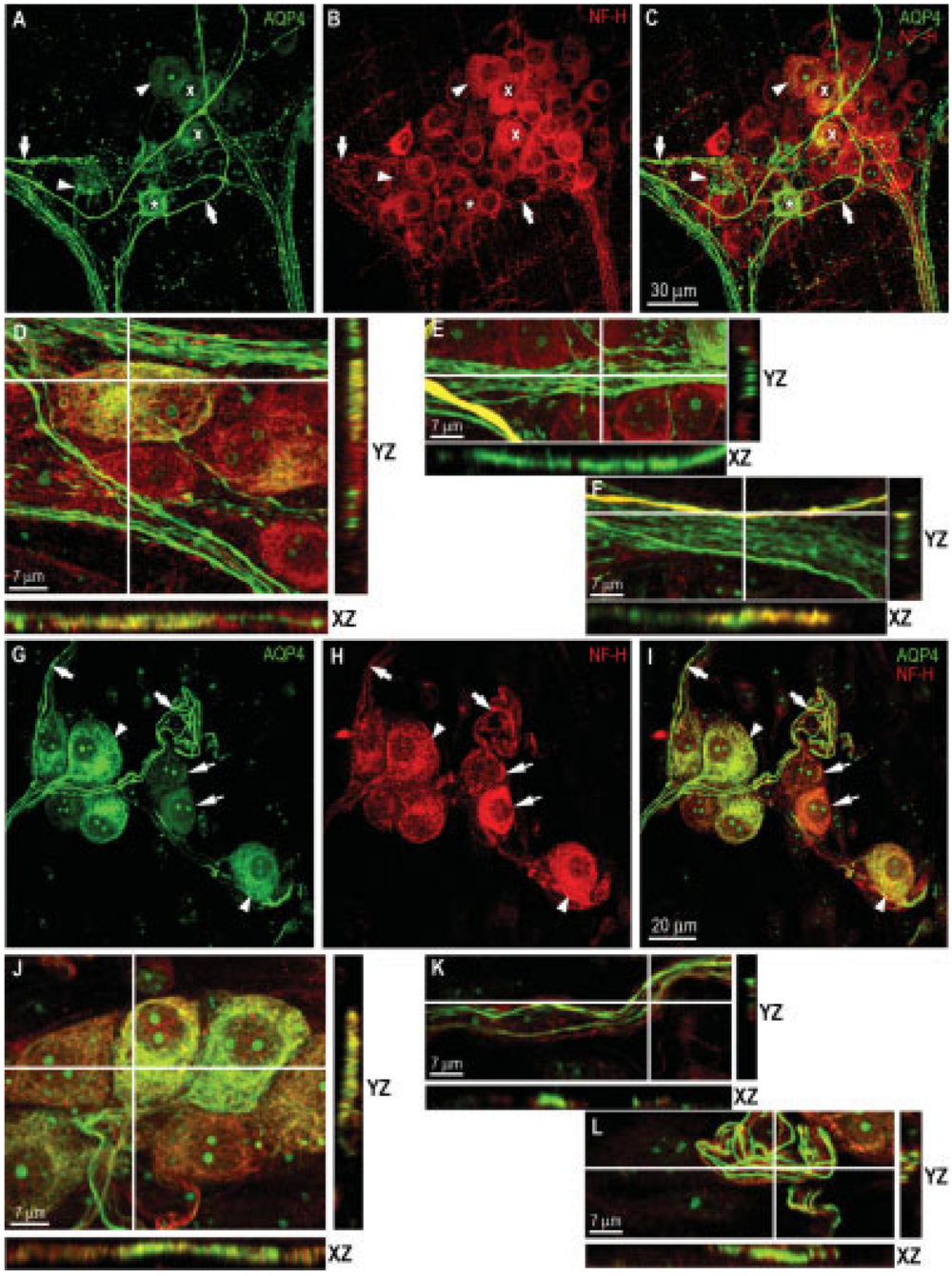

Fig. 3.

Double labeling for AQP4 (Santa Cruz Biotechnology) and the neuronal marker NF-H in the myenteric and submucosal plexuses. *Myenteric plexus* — **A**: Neurons (arrowheads) and nerve fibers (arrows) were labeled for AQP4 (*****Dogiel type I neuron). **B**: Staining for NF-H of the same field as in A. **C**: Merging of A and B showing colocalization of AQP4 and NF-H in some neurons (x). Scale bar = 30 µm. **D**: Cross-sectional analysis of confocal stacked images exhibiting occasional colocalization of AQP4 and NF-H in some neurons (*XY* and *YZ* views). **E**: Cross-sectional analysis of nerve fibers showing AQP4 uniformly distributed along internodal nerve fiber strands. (**F**) Occasional colocalization of AQP4 and NF-H observed in some nerve fiber strands. Scale bar = 7 µm. *Submucosal plexus* — **G**: Neurons (arrowheads)

and nerve fibers (arrows) in the ganglia clearly labeled for AQP4. **H**: Staining for NF-H showing that most neurons were AQP4 positive. Neurons in the two layers of the submucosal plexus (denoted by arrowheads and thin arrows) exhibited a similar distribution of AQP4. **I**: Merging of G and H illustrating that most submucosal neurons (arrowheads) and some nerve fibers (arrows) coexpressed AQP4 and NF-H. Scale bar = 20 μm. **J**: Cross-sectional analysis of confocal stacked images exhibiting abundant colocalization of AQP4 and NF-H in most submucosal neurons (*XZ* and *YZ* views). **K**: Most nerve fibers evenly expressed AQP4. **L**: In rare cases AQP4 colocalized with NF-H in some nerve fibers. Scale bar = 7 μm. [Color figure can be viewed in the online issue, which is available at www.interscience.wiley.com.]

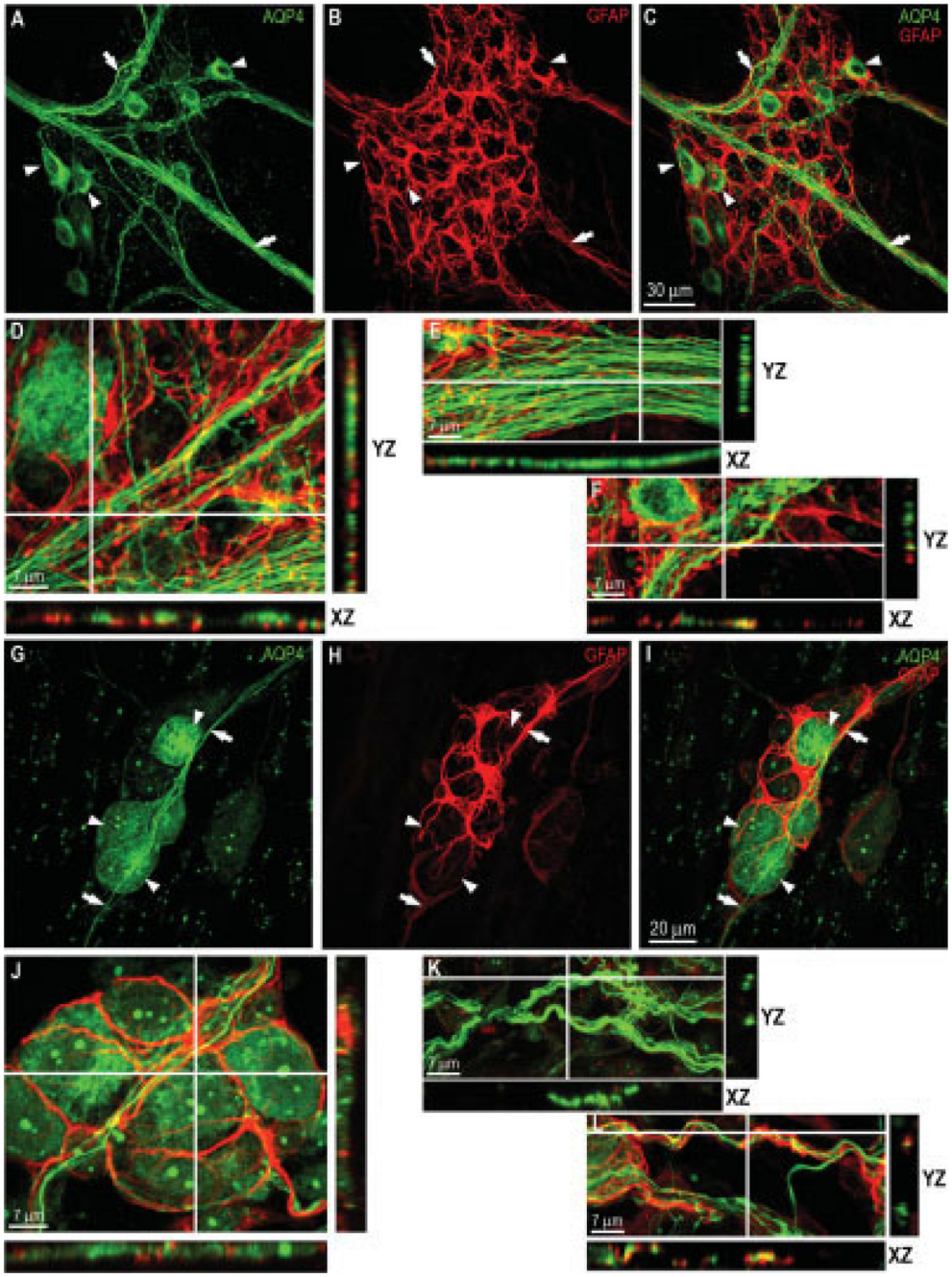

Fig. 4.

Double labeling of myenteric plexus using AQP4 (Santa Cruz Biotechnology) and the glial marker GFAP in myenteric and submucosal plexuses. *Myenteric plexus* — **A**: Some neurons (arrowheads) in the ganglion and nerve fiber strands (arrows) were labeled for AQP4. **B**: Staining for GFAP of the same field as in A; enteric glial cell network and their processes were GFAP positive. These cells are in the space between the neurons. **C**: Merging of A and B illustrating that neurons, not glial cells, were the only cells that expressed AQP4 in the myenteric plexus. Scale bar = 30 µm. **D**: Cross-sectional analysis of confocal stacked images showing that AQP4-positive neurons were surrounded by a dense network of glial cell bodies and cell processes. **E**: Uniform distribution of AQP4 along nerve fibers. **F**: Some colocalization

of AQP4 and GFAP observable where nerve fibers came into close contact with glia cell processes. Scale bar =7 μm. *Submucosal plexus* — **G**: Numerous neurons (arrowheads) and nerve fibers (arrows) were AQP4-positive. **H**: Staining of the same field for GFAP revealing glial cells in the space between the neurons. Glial cells lacked AQP4 immunoreactivity. **I**: Merging of G and H confirming separation of the staining. Scale bar = 20 μm. **J**: Cross-sectional analysis of confocal stacked images demonstrating that AQP4-positive cells were indeed neurons, not glial cells. **K**: Nerve fibers in the submucosal plexus showing uniform distribution of AQP4, similar to that of myenteric plexus. **L**: Apparent colabeling of some nerve fibers for GFAP could be a result of the presence of glial processes. Scale bar = 7 μm. [Color figure can be viewed in the online issue, which is available at www.interscience.wiley.com.]

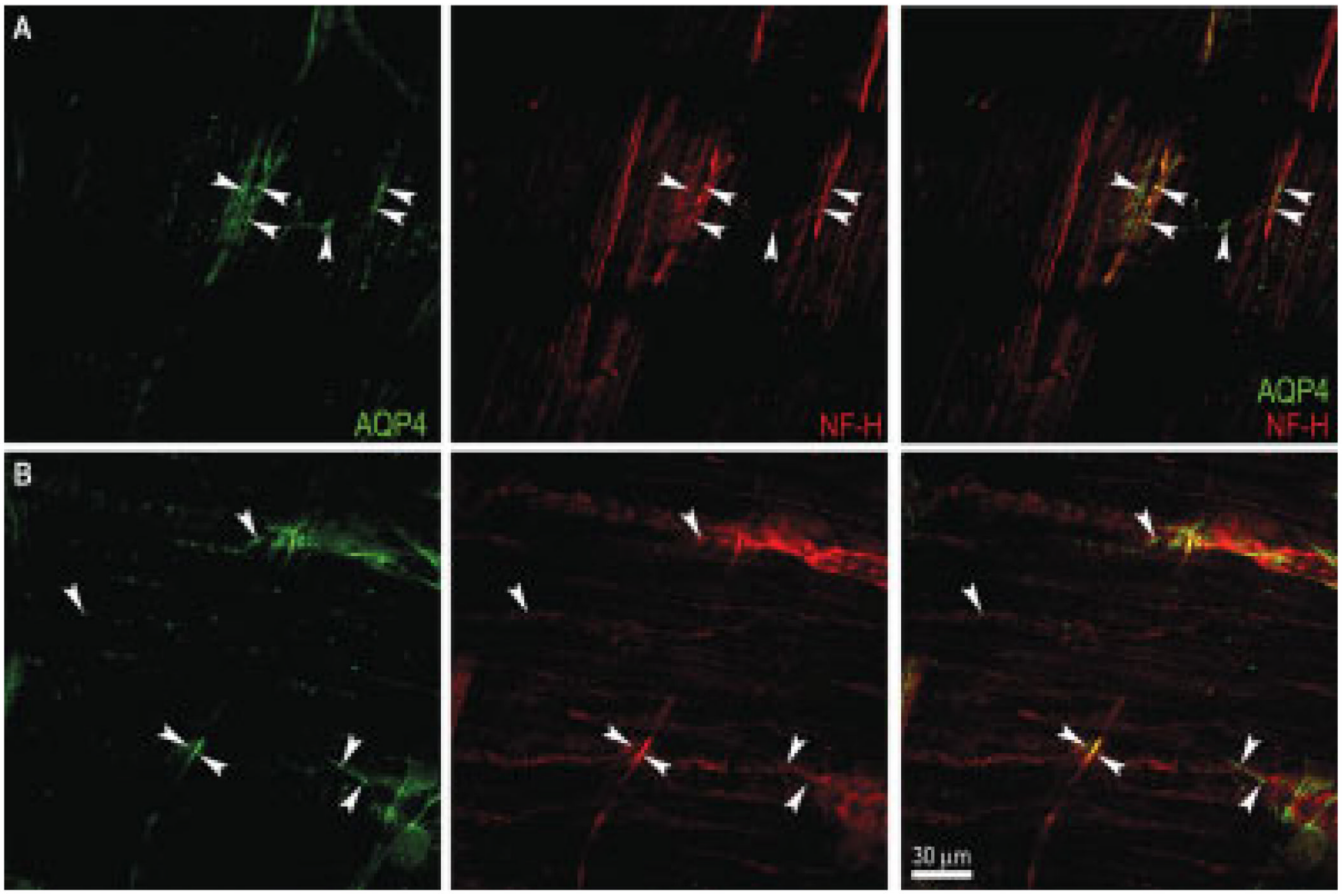

Fig. 5.

Serial confocal images showing AQP4-containing nerve fibers in muscle of mouse colon. **A**: AQP4-positive nerve fibers (arrowheads) in the longitudinal muscle layer. **B**: AQP4-positive nerve fibers (arrowheads) in the circular muscle layer. Scale bar = 30 µm. [Color figure can be viewed in the online issue, which is available at www.interscience.wiley.com.]

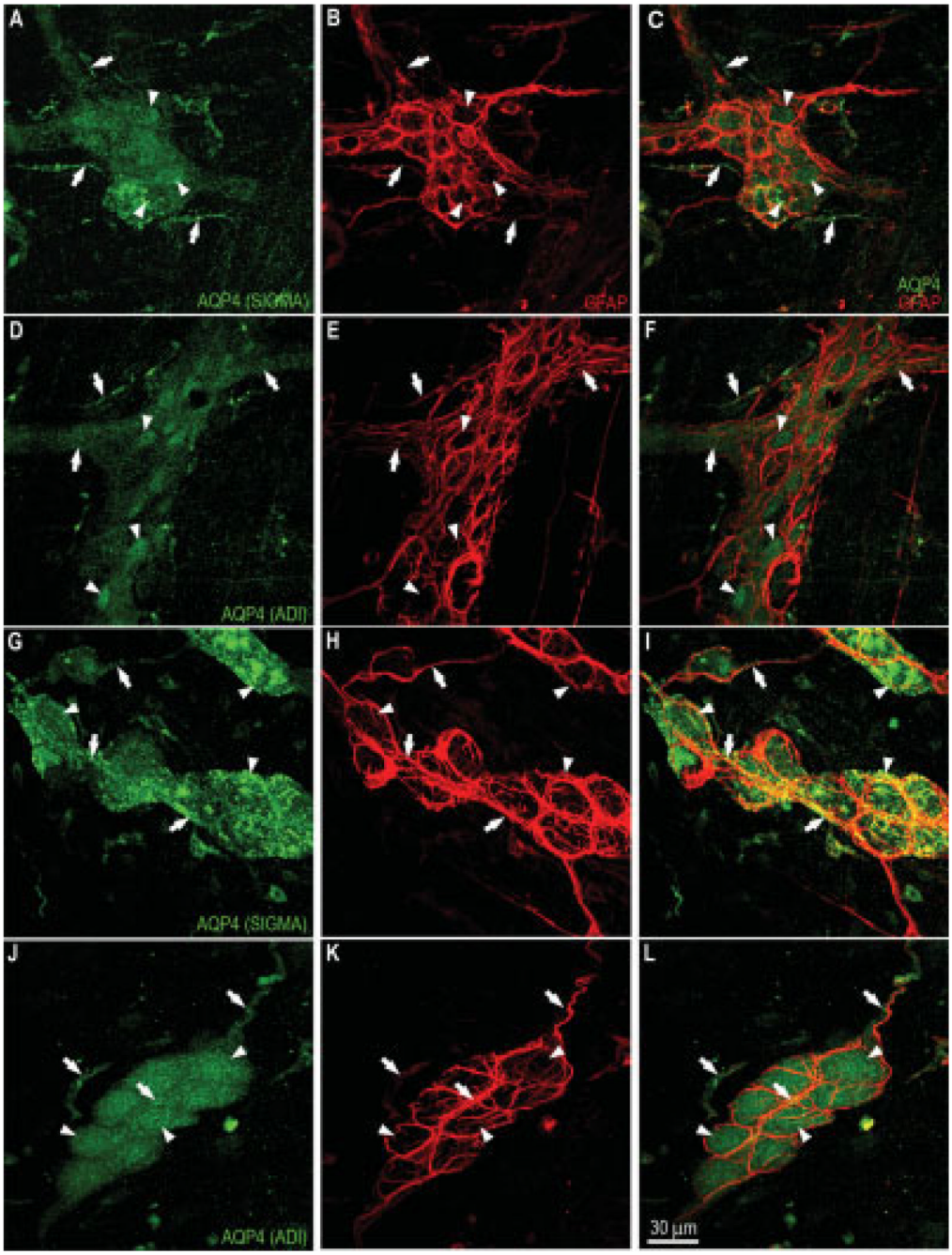

Fig. 6.

Additional AQP4 staining of myenteric and submucosal plexuses in the mouse colon using rabbit polyclonal antibodies against rat AQP4 (Sigma-Aldrich and Alpha Diagnostic International). *Myenteric plexus* — **A**: Some neurons (arrowheads) in the ganglion and nerve fiber strands (arrows) were diffusely labeled for AQP4 using Sigma-Aldrich antibody. **B**: Staining for GFAP of the same field as in A. **C**: Merging of A and B illustrating that neurons, not glial cells, were positively labeled for AQP4. **D**: Several neurons (arrowheads) and nerve fibers (arrows) were positively stained for AQP4 using Alpha Diagnostic International antibody. **E**: GFAP expression of the same field as in D. **F**: Merging of D and E showing AQP4 distribution similar to that in C. *Submucosal plexus* — **G**: Punctate AQP4 expression in neurons

(arrowheads) and some nerve fibers (arrows) detected using Sigma-Aldrich antibody. **H**: Staining of the same field for GFAP. **I**: Merging of G and H showing glial cells in the space between neurons. **J**: Numerous neurons (arrowheads) and nerve fibers (arrows) were positively labeled for AQP4 using Alpha Diagnostic antibody. **K**: Staining for GFAP of the same field. **L**: Merging of J and K illustrating punctate distribution of AQP4 similar to that in I. Scale bar = 30 μm. [Color figure can be viewed in the online issue, which is available at www.interscience.wiley.com.]

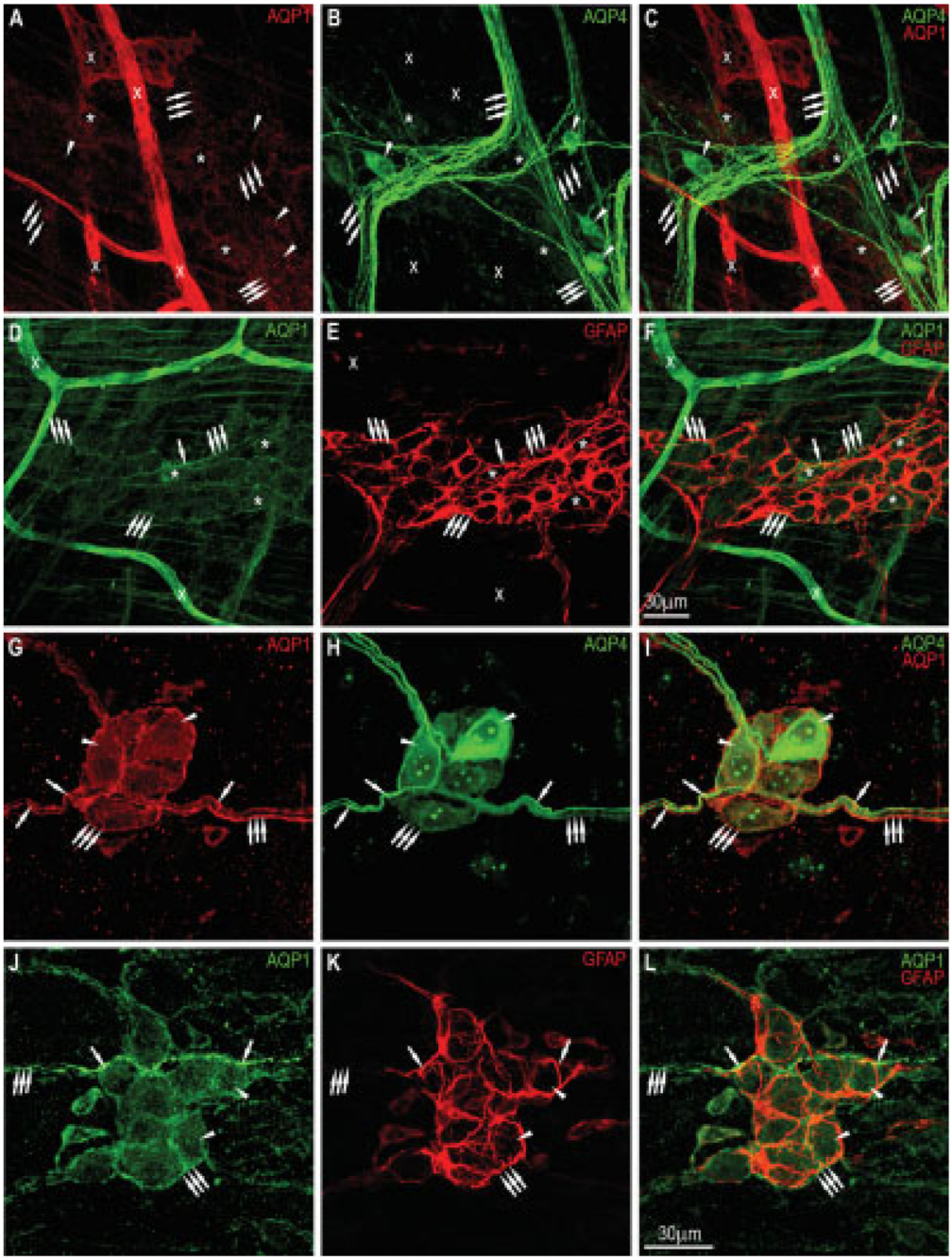

Fig. 7.

Double labeling of AQP1 (Alpha Diagnostic International) and AQP4 (Santa Cruz Biotechnology) in the myenteric and submu-cosal plexuses of the mouse colon. *Myenteric plexus* — **A, D**: Some neurons (asterisks) and nerve fibers (thin arrows) were lightly positive for AQP1. Blood vessels (x) were brightly stained for AQP1. **B**: AQP4 expression of neurons (thin arrows) and nerve fibers in the same field. **C**: Merging of A and B showing very little or no colocalization of AQP1 and AQP4. **E**: Staining for GFAP of the same field as in D showing glial cell network and their processes. **F**: Merging of D and E indicating that only neurons were AQP1 positive. Scale bar = 30 µm. *Submucosal plexus* — **G, J**: Many neurons (arrowheads) and nerve fibers (arrows) express abundant AQP1. **H**: AQP4 expression in the neurons

(arrowheads) and nerve fibers (arrows) in the same field as in G. **I**: Merging of G and H shows moderate colocalization of AQP1/AQP4 in neurons (arrows) and along the nerve fibers (single arrows). **K**: Staining for GFAP of the same field as in J. **L**: Merging of J and K demonstrates numerous colocalizations of AQP1 and GFAP where glial cell processes are in close contact with nerve fibers (single arrows). Scale bar = 30 μm. [Color figure can be viewed in the online issue, which is available at www.interscience.wiley.com.]

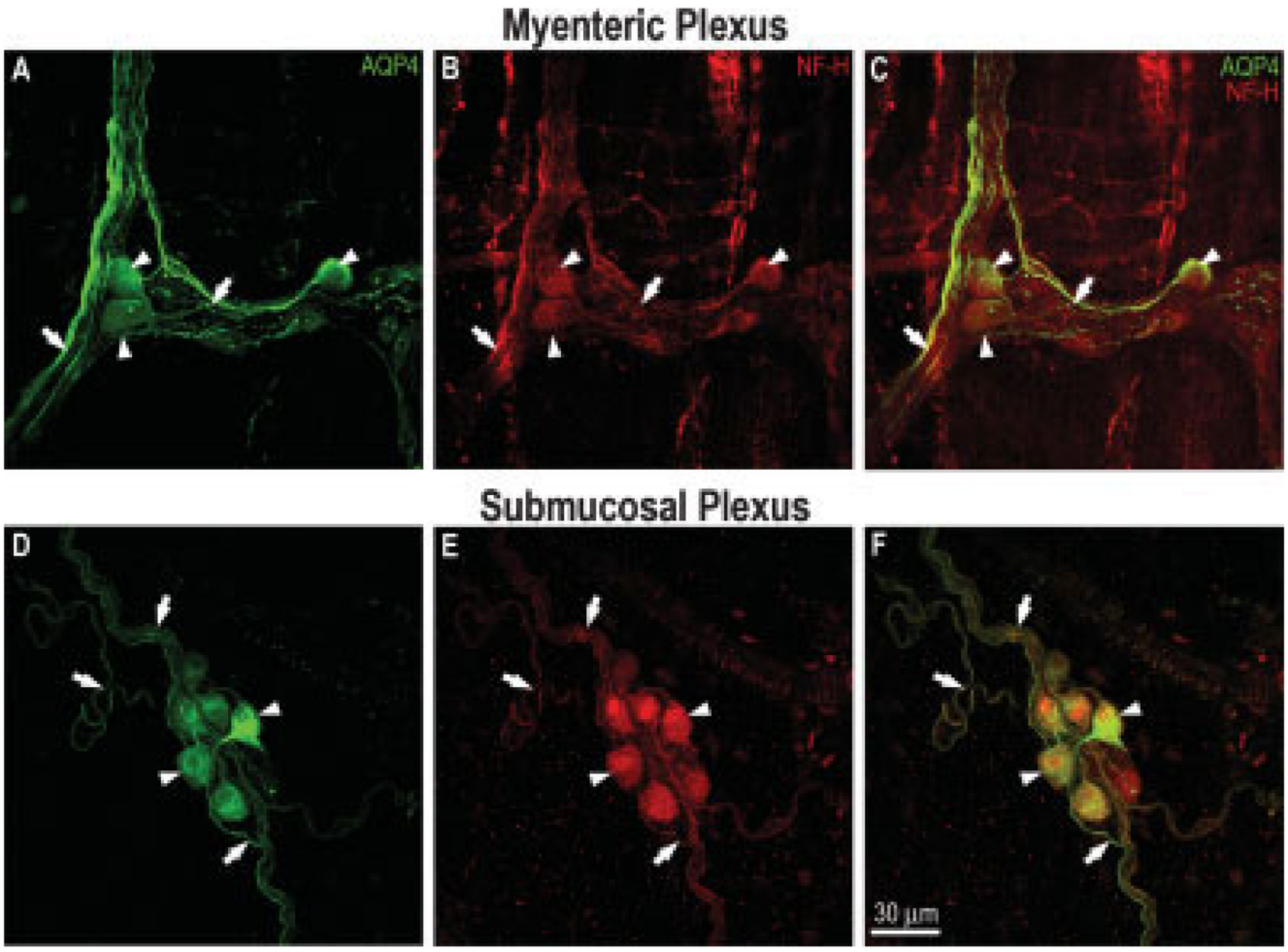

Fig. 8.

Double labeling for AQP4 (Santa Cruz Biotechnology) and NF-H in the myenteric and submucosal plexuses of the rat colon. *Myenteric plexus* — **A**: Neurons (arrowheads) and nerve fibers (arrows) in the ganglia clearly labeled for AQP4. **B**: Staining for NF-H showing that the AQP4-positive cells are neurons. **C**: Merging of A and B indicating that most myenteric neurons (arrowheads) and some nerve fibers (arrows) coexpress AQP4 and NF-H. *Submucosal plexus* – **D**: Numerous neurons (arrowheads) and several nerve fibers (arrows) richly stained for AQP4. **E**: NF-H expression of the same field as in D indicating that almost all submucosal neurons were labeled for AQP4. **F**: Merging of D and E demonstrating extensive colocalization of AQP4 and NF-H in the rat submucosal plexus. Scale bar = 30 µm. [Color figure can be viewed in the online issue, which is available at www.interscience.wiley.com.]

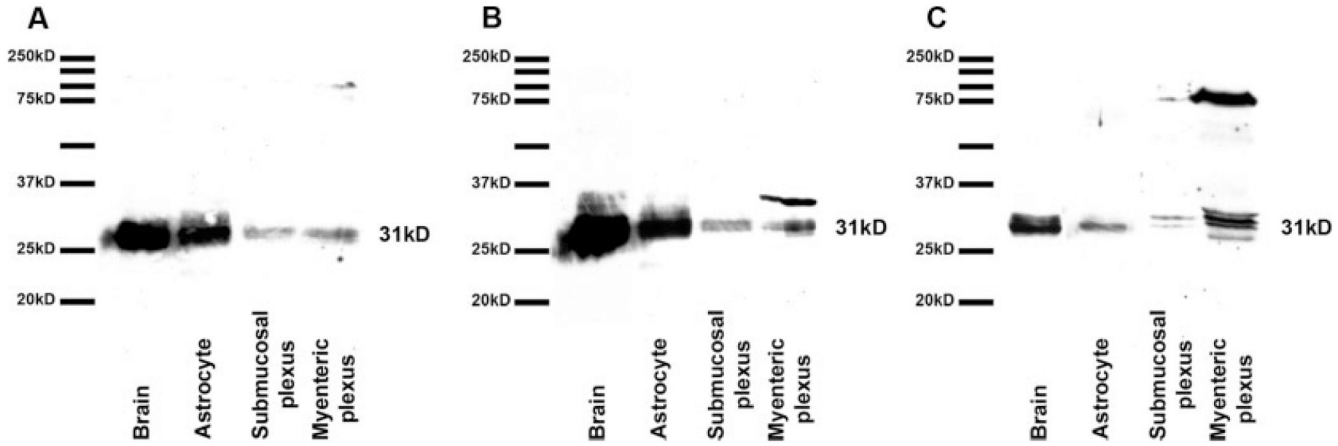

Fig. 9.

Western blot analysis was performed to determine AQP4 expression in submucosal and myenteric plexuses of mouse colon using brain and astrocytes as positive controls. Tissue samples were collected from the same C57BL/6J animals, and astrocytes were cultured from neonatal C57BL/6J mice. The samples were probed using (**A**) goat polyclonal antibody against human AQP4 (Santa Cruz Biotechnology), (**B**) rabbit polyclonal antibody against rat AQP4 (Sigma-Aldrich), and (**C**) rabbit polyclonal antibody against rat AQP4 (Alpha Diagnostic International). Both myenteric and submucosal plexuses expressed doublets at around 31 kDa.

TABLE 1

Distribution of AQP4 Positive Neurons with Respect to NF-H Positive Neurons in the Myenteric and Submucosal Plexuses of Mouse and Rat Colons.

	Myenteric plexus				Submucosal plexus			
	Ganglia	**AQP4**	**NF-H**	**AQP4/NF-H (%)**	**Ganglia**	**AQP4**	**NF-H**	**AQP4/NF-H (%)**
Mouse # 1	22	41	377	11	15	62	73	85
Mouse # 2	32	128	964	13	39	137	184	74
Mouse # 3	26	75	648	12	33	120	145	83
Mouse # 4	26	80	784	10	33	136	180	76
Mouse # 5	31	101	807	13	28	191	147	77
Average				12 ± 1				79 ± 5
Rat # 1	31	81	649	12	32	154	202	76
Rat # 2	33	105	674	16	29	146	188	80
Rat # 3	35	91	796	11	32	184	228	81
Average				13 ± 2				79 ± 2